INTERACTION OF K^+ ION WITH THE SOLVATED GRAMICIDIN A TRANSMEMBRANE CHANNEL

KWANG S. KIM,* D. P. VERCAUTEREN,‡ M. WELTI,* S. CHIN,* AND E. CLEMENTI*
IBM Corporation, Department 48B, Mail Station 428, Kingston, New York 12401; and the ‡National Foundation for Cancer Research, Bethesda, Maryland 20814

ABSTRACT Using Urry's gramicidin A (GA) atomic coordinates and ab intio calculations, the interaction energies of a K^+ ion with GA are examined. From these energies the values of the fitting parameters are obtained for 6-12-1 atom-atom pair potentials. The potential of the GA channel as experienced by the ion is analyzed in detail. An energy profile of the K^+ ion in the GA channel is obtained by analyzing iso-energy maps. Using Monte Carlo simulations, the energy profiles of the K^+ ion with the solvated GA channel are analyzed and the hydration structures in the presence of the K^+ ion are studied.

INTRODUCTION

As transmembrane channels play key roles for bio-mechanism, the understanding of their microscopic mechanism is very important in order to learn about their real activities in living cells. Accordingly, much effort has been devoted to discovering the structures and properties of the ion conducting form of gramicidin both by experimental and theoretical approaches. For recent reviews, see Urry (1) and Ovchinnichov (2).

We recall that the primary structure of gramicidin (GA) is HCO—L-Val[1]—Gly[2]—L-Ala[3]—D-Leu[4]—L-Ala[5]—D-Val[6]—L-Val[7]—D-Val[8]—L-Trp[9]—D-Leu[10]—L-Trp[11] — D-Leu[12] — L-Trp[13] — D-Leu[14] — L-Trp[15] — $NHCH_2$—CH_2OH. In Fig. 1 we show a GA membrane channel. In the top-left inset, a GA channel consisting of a GA dimer is surrounded by phospholipid membranes. In the top-right inset, a GA monomer is projected onto the x-y plane (the z axis lies along the axis of the channel), and the 15 amino acid residues of GA are explicitly labeled. In the bottom-left inset two GA monomers are projected onto the x-y plane, while in the bottom-right inset they are projected onto the x-z plane.

Previously, we reported (3) the potential energy and structure of water molecules interacting with a GA channel, modeled according to Urry's atomic coordinates (4). This paper will report the interaction energy of K^+ with GA using ab initio calculations, and analyze the iso-energy contour maps in order to understand the strengths and locations of the binding sites within the channel. Using Monte Carlo (MC) simulations, we will also investigate (a) the number of molecules that can be placed inside the GA channel, (b) the energy profiles of a K^+-H_2O-GA system and (c) the structure of the water molecules inside the channel in the presence of a K^+ ion.

INTERACTION ENERGY OF A K^+ ION WITH A GA CHANNEL

To obtain a realistic interaction between a K^+ ion with GA, the atom-atom pair potentials of a K^+ ion interacting with amino acids or with a polypeptide chain have been derived from ab initio calculations (SCF-LCAO-MO approximation) computed at more than 1,300 conformations. For the ab initio SCF computation, we used a minimal basis set, consisting of seven s-type Gaussian functions and three p-type Gaussian functions for the nonhydrogen atoms (5). For the hydrogen atoms, we used four s-type functions (5), mainly to decrease the basis set superposition error (6, 7). As a matter of fact, this superposition error was negligible for the interaction energy of a K^+ ion with the fragments of GA; therefore, we did not consider this superposition error in our calculation.

Once having obtained the ab initio interaction energies, we fitted them to an analytic potential energy function

$$E = \Sigma_j[-A(j,a)/r(j)^6 + B(j,a)/r(j)^{12} + C(j,a)q(j)/r(j)],$$

where j designates an atom of GA and $r(j)$ is the distance from the K^+ ion (with a charge equal to 1) to the jth atom, with charge $q(j)$. Here we select another set of indices "a" to further characterize the atom of GA interacting with a K^+ ion. This indice "a" designates the classes within a group of atoms of equal atomic number. A class characterizes the electronic environment of the jth atom within the molecule. This characterization is obtained by selecting as criteria (a) the atomic number, (b) the hybridization of the

Dr. Vercauteren's present address is Laboratoire de Chimie Theorique Appliquee, Faculties Universitaires Notre-Dame de la Paix, B-5000 Namur, Belgium.

Dr. Welti's present address is Laboratorium fur Organische Chemie, ETH-Zentrum, CH-8092 Zurich, Switzerland.

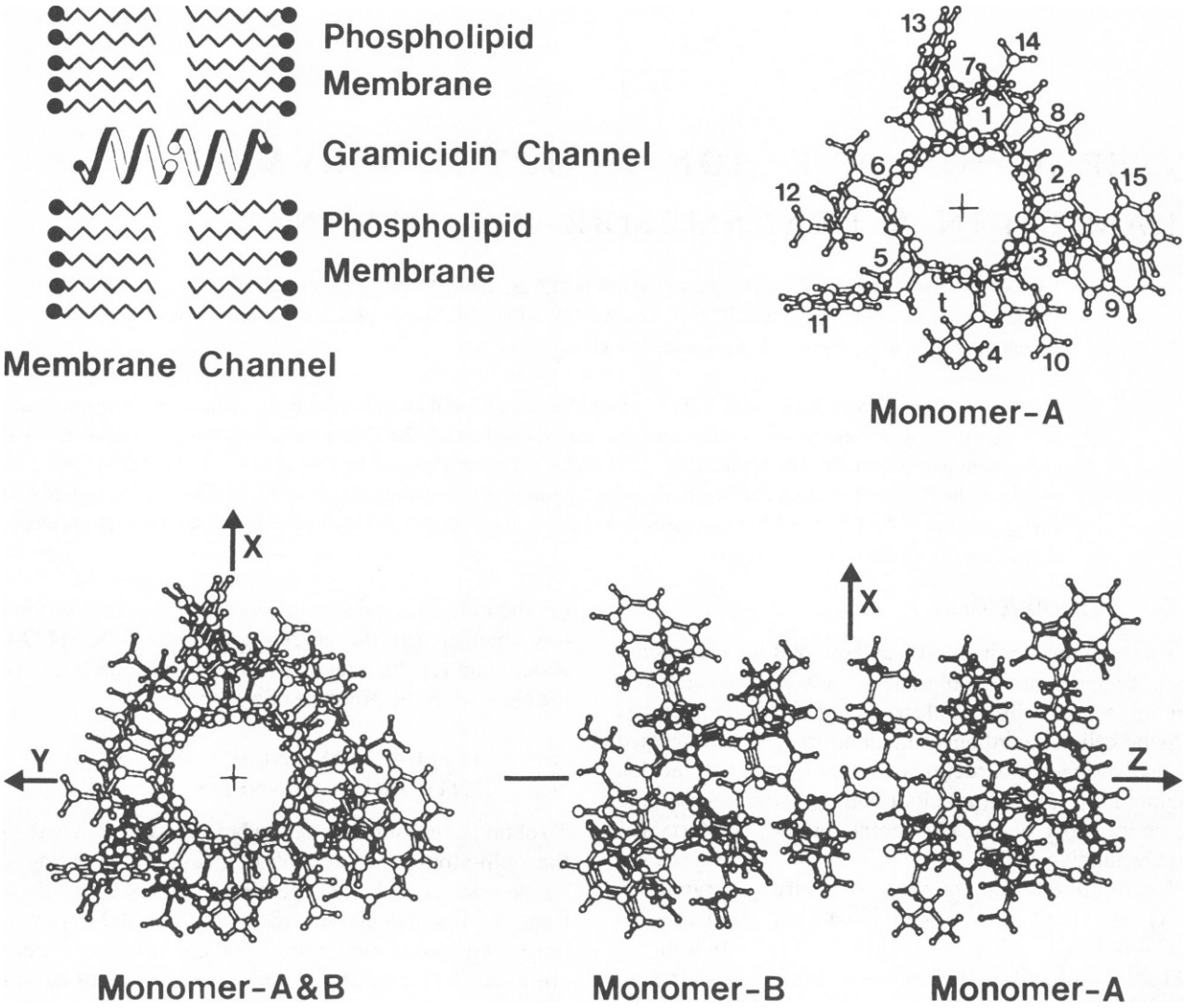

FIGURE 1 Features of a GA membrane channel. *Top left*: schematic representation of a membrane channel. *Top right*: projection of a GA monomor onto *x-y* plane with labels for the 15 residues. *Bottom*: projections of a GA channel (GA dimer) onto *x-y* plane (*left*) and *x-z* plane (*right*).

atom (number of bonds), (*c*) the net atomic charge (8), and (*d*) the energy difference between the atom in the molecule and the isolated atom, i.e., the molecular orbital valency state (MOVS) energy (7).

In Figs. 2 and 3 and Table I we show how the classes are characterized, reporting the net charges (in electrons), the MOVS (in hartrees), and the class index. Table I also reports the A, B, and C coefficients of the 6-12-1 analytical potential energy function mentioned above. The fitting of the ab initio interaction energies to obtain the above analytical atom-atom pair potentials, was carried out to a mean SD of 1.5 kcal/mol. The overall quality of the fitting is shown by the standard plot (fitted/ab initio) of Fig. 4.

In Fig. 5, we report iso-energy maps for the L-Ala, L-Val, D-Val, D-Leu, L-Trp residues, the ethanolamine ($HOC—NH—CH_2—CO—NH—CH_2—CH_2OH$) tail and the two central formyl heads. For each molecular component two plots are given. First, the one in two dimensions contains an ORTEP projection of the amino acid into the selected plane. The second representation is three dimensional; it shows explicitly both the attractive site minima and the repulsive regions (which have the appearance of mesa because the repulsive energies have been cut off at 6 kcal/mol). The contour-to-contour interval is 2 kcal/mol. From these figures, note that the D-Leu and L-Trp residues show strong interactions with the K^+ ion.

In a similar fashion, we have obtained the iso-energy contour maps for a plane bisecting the GA channel, as shown in Fig. 6. The bottom inset is the iso-energy map for the *x-z* projection of the entire channel and the regions at the two extrema extending up to $Z = \pm 47$ atomic unit. The top inset is the iso-energy map for the *y-z* projection. Notice that the channel is helical and the difference between the *x-z* and *y-z* projections is not significant.

A detailed view of the channel energetics is given in Fig.

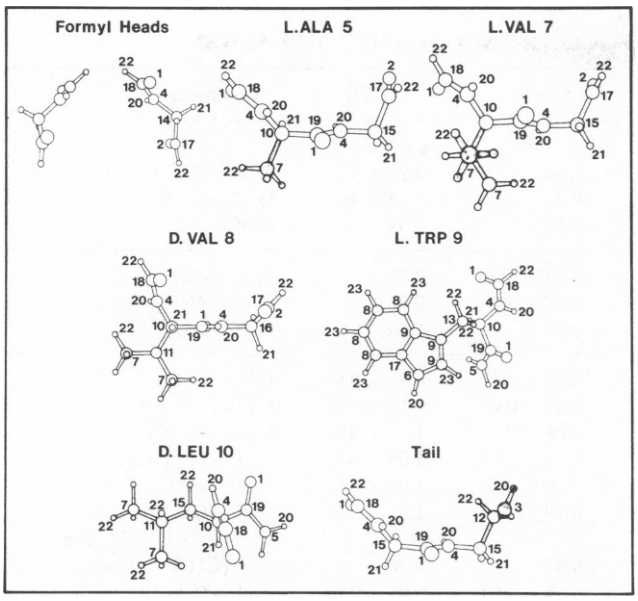

FIGURE 2 Classes for each atom of GA.

7. At the upper part of the figure, eight iso-energy maps are reported for the cross section of the channel corresponding to Z = 0, 2, 4, 8, 11, 12, 13, and 14 Å. Near the so-called binding sites (1) (i.e., near Z = 11 Å), the effective cross section of the channel (along the Z axis) is the smallest. Therefore, near this region, the libration mechanism of the GA carbonyl groups is expected to play a very important role.

At the bottom of the Fig. 7 we show a graph giving the lowest energy determined in each x-y cross section. Notice the very prominent minima inside the channel. The strong interaction energies of K^+ with GA are mainly due to the carbonyl oxygens rather than the residue effects. The interaction energy of K^+ with one carbonyl oxygen is about -20 kcal/mol at the most favorable position of K^+. The K^+/GA interaction energy can be as large as -54 kcal/mol by summing over all the carbonyls of GA, because the interactions of K^+ with 30 carbonyl oxygens in GA are all additive (mainly by coulomb interaction energies). When the K^+ ion is near the center of the channel, the interaction energy is stronger because the carbonyls are closer to the K^+ ion than in other cases.

Before reporting our MC simulation results, we will discuss one more detail at the single ion level. In Fig. 8, we compare cylindrical iso-energy maps, obtained by selecting cylinders with a radius of 2.0 and 2.5 atomic units, with the figure of the helical GA backbone on the right. The hard core region appears to be conspicuous even in the map of R = 2.0 atomic units. This implies that the K^+ ion can only move through the channel along the path near the Z axis.

MONTE CARLO SIMULATIONS

In this section we describe features of our simulation that follow Metropolis Monte Carlo modeling (9). We performed MC simulations for the K^+-H_2O-GA system, attempting to find the energy profiles of the system and the effect of the K^+ ion on the water conformations. In all simulations the selected temperature is 300° K, and the K^+ ion and the water molecules are free to move. We placed 81 water molecules in a cylindrical volume, whose length and radius are 48 and 5.5 Å, respectively. With the above

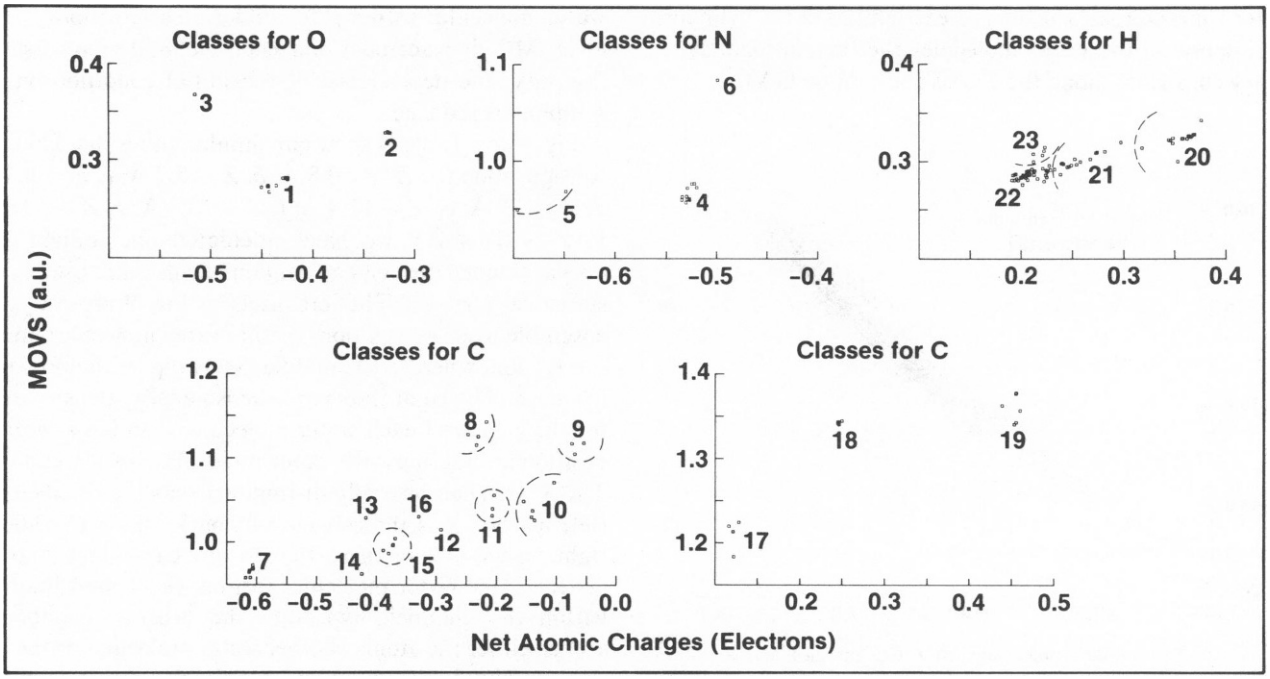

FIGURE 3 Description of each class in terms of atom, MOVS, and net atomic charges.

TABLE I
DESCRIPTION OF CLASSES INCLUDING COEFFICIENTS, NET CHARGE, AND MOVS*

Atom class		A	B	C	Charge	MOVS	Comment
					e	*atomic unit*	
O	1	0.7357*E* + 01	0.1641*E* + 06	0.1067*E* + 01	−0.44 ± 0.01	0.28 ± .01	O of =C=O
	2	0.2558*E* + 03	0.1896*E* + 06	0.9021*E* + 00	−0.33 ± 0.02	0.33 ± .01	O of =C=O
	3	0.6916*E* + 01	0.1746*E* + 06	0.9025*E* + 00	−0.51	0.37	O of —OH
N	4	0.6246*E* + 01	0.3669*E* + 06	0.9094*E* + 00	−0.53 ± .01	0.97	N of —(NH)—
	5	0.1894*E* + 04	0.6918*E* + 06	0.9724*E* + 00	−0.67 ± .02	0.96	N of —(NH)—
	6	0.6753*E* + 01	0.3784*E* + 06	0.9100*E* + 00	−0.50	1.08	N of L-Trp
C	7	0.7012*E* + 01	0.1528*E* + 07	0.9092*E* + 00	−0.61 ± 0.01	0.97 ± 0.01	C of —CH_3
	8	0.6436*E* + 01	0.9464*E* + 06	0.9074*E* + 00	−0.23 ± 0.01	1.13 ± 0.01	C of L-Trp ring
	9	0.6101*E* + 01	0.8326*E* + 06	0.9004*E* + 00	−0.06 ± 0.01	1.11 ± 0.01	C of L-Trp ring
	10	0.6257*E* + 01	0.4136*E* + 07	0.9011*E* + 00	−0.13 ± 0.02	1.05 ± 0.02	C of —(C_α HRes.)—
	11	0.6035*E* + 01	0.8427*E* + 07	0.9003*E* + 00	−0.20 ± 0.01	1.04 ± 0.01	C of —CHR_2
	12	0.6852*E* + 01	0.4166*E* + 07	0.1019*E* + 01	−0.29	1.01	C of —CH_2OH of tail
	13	0.6311*E* + 01	0.2014*E* + 07	0.1080*E* + 01	−0.42	1.03	C_1—($C_\beta H_2$)— of L-Trp
	14	0.7381*E* + 01	0.2015*E* + 07	0.9409*E* + 00	−0.42	0.96	C_1—(CH_2)— of formyl
	15	0.6089*E* + 01	0.7697*E* + 06	0.9684*E* + 00	−0.38 ± 0.01	0.99 ± 0.01	C of —(CH_2)—
	16	0.9042*E* + 04	0.8443*E* + 07	0.9477*E* + 00	−0.33	1.03	C of —(CH_2)—
	17	−0.3528*E* + 04	0.3018*E* + 03	0.9100*E* + 00	0.12 ± 0.01	1.20 ± 0.02	C of =C=O, or L-Trp
	18	−0.3739*E* + 04	0.2448*E* + 06	0.9094*E* + 00	0.25 ± 0.01	1.34 ± 0.01	C of =C=O
	19	−0.5574*E* + 04	0.3010*E* + 03	0.9100*E* + 00	0.45 ± 0.01	1.36 ± 0.01	C of =C=O
H	20	0.5586*E* + 03	0.6443*E* + 05	0.1086*E* + 01	0.35 ± 0.03	0.32 ± 0.02	H connected to O,N
	21	0.7066*E* + 01	0.3000*E* + 03	0.9099*E* + 00	0.27 ± 0.03	0.30 ± 0.02	H connected to C_α
	22	0.8045*E* + 03	0.9388*E* + 05	0.9099*E* + 00	0.21 ± 0.02	0.29 ± 0.01	H connected to C
	23	0.1486*E* + 04	0.1510*E* + 06	0.9090*E* + 00	0.22 ± 0.01	0.31 ± 0.01	Aromatic H of L-Trp

*The coefficients are given so that the interaction energy and distance can be expressed in kilocalories per mole and ångströms, respectively.

choice the liquid water weight density is ~1, when the hard core volume of the GA channel is excluded from the cylinder. The water molecules are constrained to stay within the cylindrical volume. However, to ensure bulk water characteristics at the two extremities of the cylinder, we impose on the water molecules the translational symmetry constraint along the *Z* axis (but not on GA).

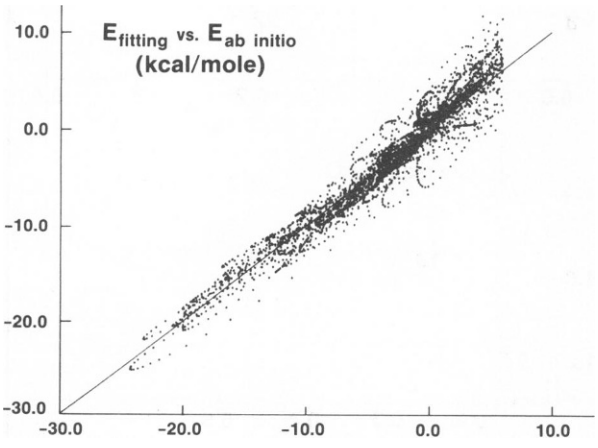

FIGURE 4 Plot of deviations between fitted energies and ab initio energies for the interaction of K^+ with GA.

Another point to consider is the possibility of a pressure difference between the right and left sides of the channel, since migration of water molecules through the channel is an unlikely event. Therefore, we allowed the rightmost water molecules to jump to the leftmost positions, if the given MC displacement is acceptable, and vice versa. In this way, the dependence of the initial condition on the sampling is reduced.

Fig. 9 and Table II show our simulation results. For each configuration (*a*, $Z = -0.8$ Å; *b*, $Z = 2.7$ Å; *c*, $Z = 6.1$ Å; *d*, $Z = 7.9$ Å; *e*, $Z = 11.4$ Å; *f*, $Z = 13.3$ Å; *g*, $Z = 15.0$ Å; *h*, $Z = 16.4$ Å), we have calculated one million MC displacements, the last half million of which are used in our statistical analysis. The left insets of Fig. 9 represent the ensemble average positions of the water molecules and of the K^+ ion, whereas the middle insets report the probability maps. The right insets are the iso-energy density maps for the energy of each water molecule or an ion at a given position interacting with water molecules, an ion and GA. The K^+ ion can be easily distinguished as the filled circles (left insets) or as the conspicuous dark region (middle or right insets). From these figures one can notice that, in general, nine water molecules form a well-bound filament within the channel, hydrating the nearest neighboring atoms: either the atoms of other water molecules or the ion, or a carbonyl oxygen atom of GA. Sometimes a water

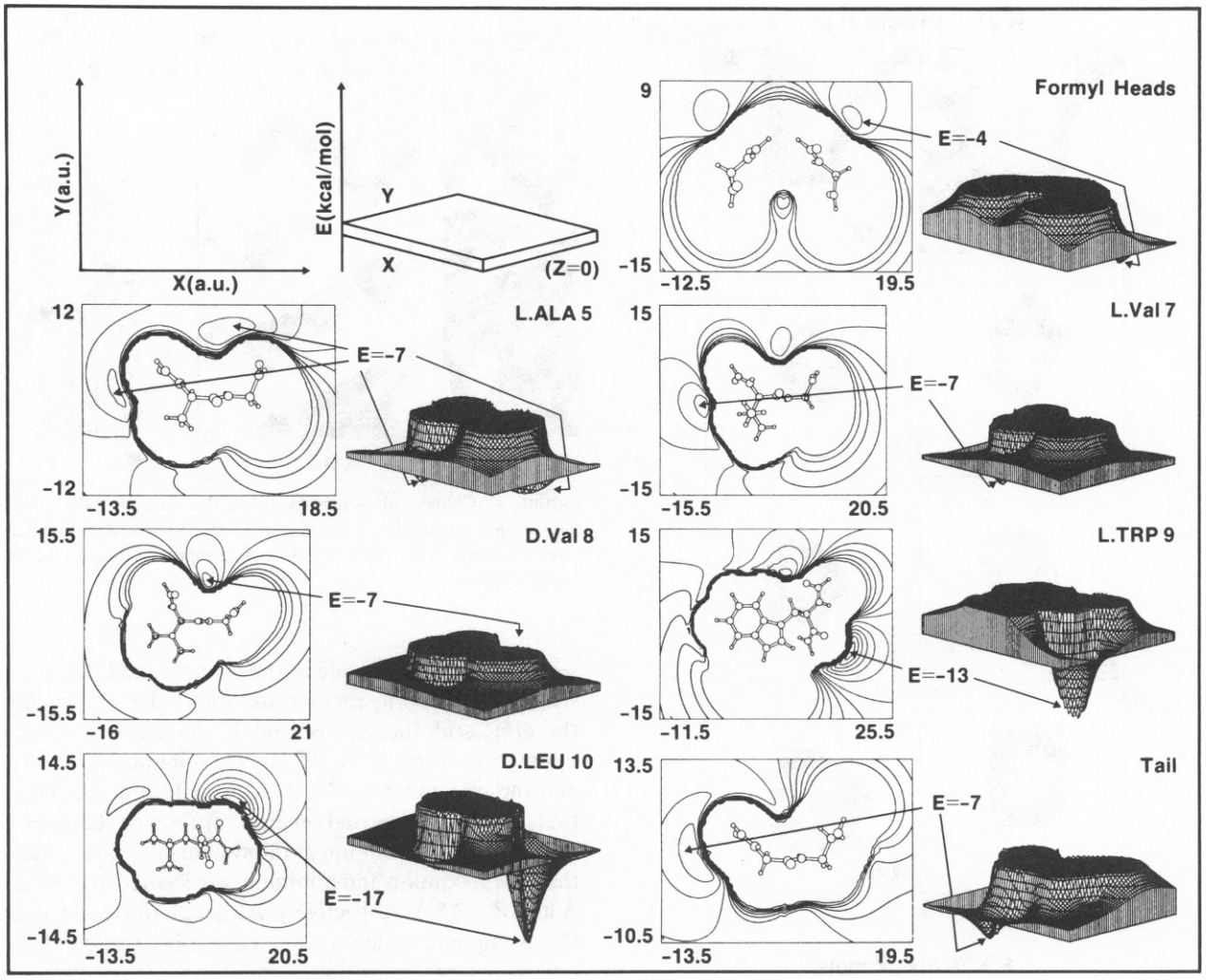

FIGURE 5 Iso-energy maps of the different GA residues including the formyl heads and ethanolamine tail interacting with K^+. Coordinates (X, Y) and interaction energies (E) are given in atomic units and kilocalories per mole, respectively.

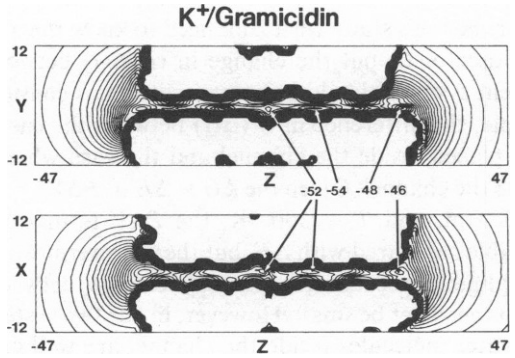

FIGURE 6 Iso-energy maps of K^+ interacting with GA. Top inset shows the cross section of $X = 0$, while bottom inset shows the cross section of $Y = 0$. Coordinates (X, Y, Z) and interaction energies (E) are given in atomic units and kilocalories per mole, respectively.

molecule inside the channel is not hydrogen bonded to its neighboring water molecule. On the other hand, as can be inferred from the probability-density maps, the water molecules at the two extremities of the cylinder begin to show somewhat bulklike characteristics.

In Table II we report the average Z position of the K^+ ion, the total energy of the system (Tot) (for 81 water molecules, one K^+ ion and the GA channel), the total interaction energy (K^+/T) of the K^+ ion with GA (K^+/GA) and with water (K^+/W), the total interaction energy (W/T) of water with GA (W/GA) and with water (W/W), and the standard deviation (SD) of the ion coordinate. We note, from the SD, that an ion outside the channel is more mobile than the one inside the channel.

In Fig. 10, we show the energy profiles for the system as obtained from the Monte Carlo simulations: K^+/GA, K^+/W, K^+/T, and Tot. Since we define $K^+/T = K^+/GA + \frac{1}{2}K^+/W$, $W/T = W/W + W/GA + \frac{1}{2}W/K^+$ and $W/K^+ = K^+/W$, the interaction energy between K^+ and

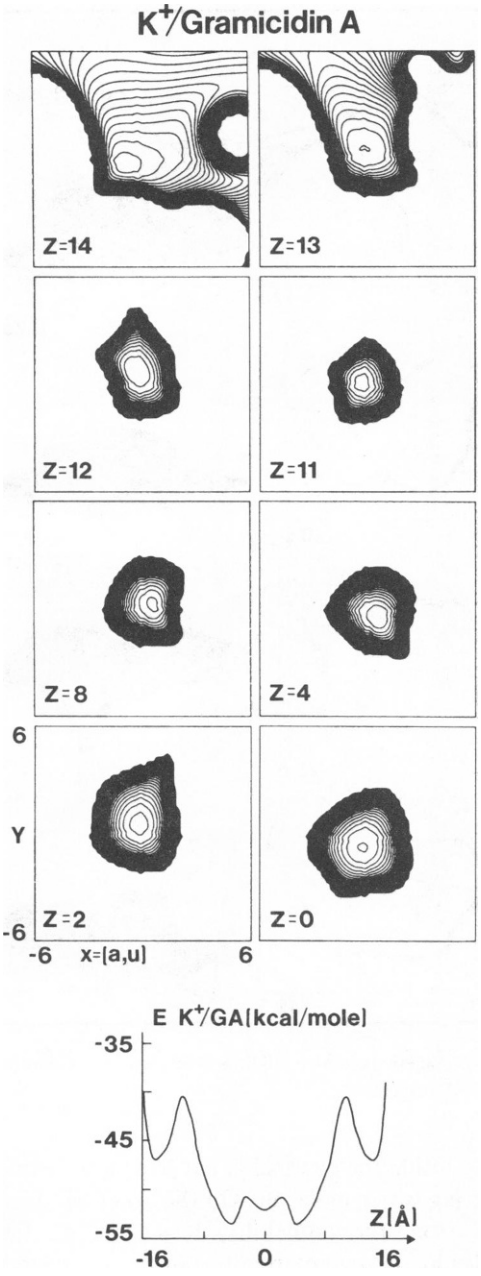

FIGURE 7 Iso-energy maps of K^+ interacting with GA in x-y projection along Z axis (for Z = 0, 2, 4, 8, 11, 12, 13, and 14 Å), and the energy profile of K^+-GA system. Z coordinates are in ångström, while X and Y coordinates are in atomic units.

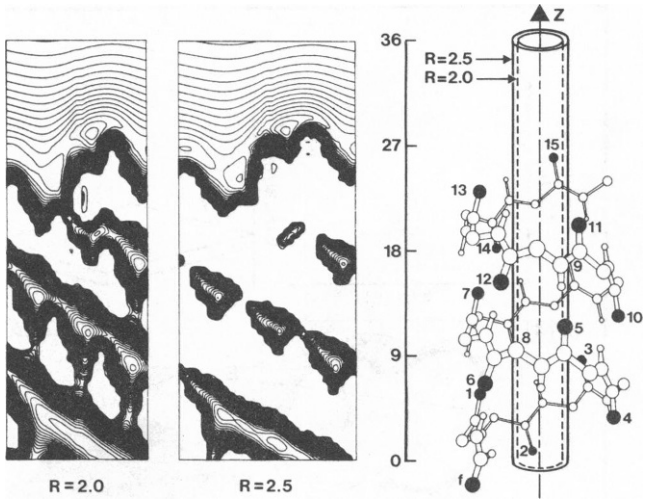

FIGURE 8 Cylindrical iso-energy maps flattened out; the cylinder's radii are R = 2.0 and R = 2.5 atomic units, respectively. Z coordinates are given in atomic units. The *right* inset is a representation of the helical backbone only.

water has been reported as $\frac{1}{2}K^+/W$. Note that the dotted line, denoted by (K^+/GA) in the figure is the energy profile obtained from the iso-energy maps (see the bottom inset of Fig. 7). Therefore, the latter does not include the thermal effect for K^+, whereas the solid line denoted by K^+/GA includes it. Fig. 10 and Table II show that the interaction energy of K^+/GA is stronger inside the channel than outside the channel, while the interaction energy of K^+/W is just the opposite. This is as expected because when K^+ is near the center of the channel the K^+ ion can strongly interact with the carbonyls at shorter distances, while when K^+ is outside of the channel the K^+ ion can be strongly solvated by many water molecules. By combining the effects of the K^+/W and K^+/GA interactions, the interaction energy of K^+/T has the minimum at Z = 14 Å and the maximum at Z = 0 Å. Finally, Fig. 10 indicates that the total internal energy difference between the maximum and minimum of the system is ~120 kJ/mol and that the maximum and minimum are located around Z = 0 Å and Z = 15 Å, respectively. Although the total energy in the asymptotic region for K^+ has not been calculated, the internal energy activation barrier for K^+ may be estimated to be < 70 kJ/mol from the energy value at Z = 16.4 Å.

DISCUSSION

To properly compare our results with the experimental results, we must consider the Gibbs free energy, G. In particular, we are interested in the location of the maximum and minimum and also in the height of the activation barrier. For this study we do not need to know the absolute magnitude of G, but the change in G (ΔG) between two different systems should be computed. Let us consider, for example, the difference in G (ΔG) between the case when K^+ is placed inside the channel and the case when K^+ is outside the channel. Given the $\Delta G = \Delta E + P\Delta V - T\Delta S$ at P = 1 atm. and T = 300 °K, the $P\Delta V$ term would be negligible compared with ΔE, but the $T\Delta S$ term would not be negligible because the entropy change between two systems need not be small. However, in our two systems the nine water molecules inside the channel are well ordered, as can be seen from Fig. 9. Therefore, the difference of ΔS between the nine water molecules of the two cases would be small. From the standard deviation of the ion coordinates (SD in Table II) we notice that the entropy difference due to K^+ between the two cases will be different: in

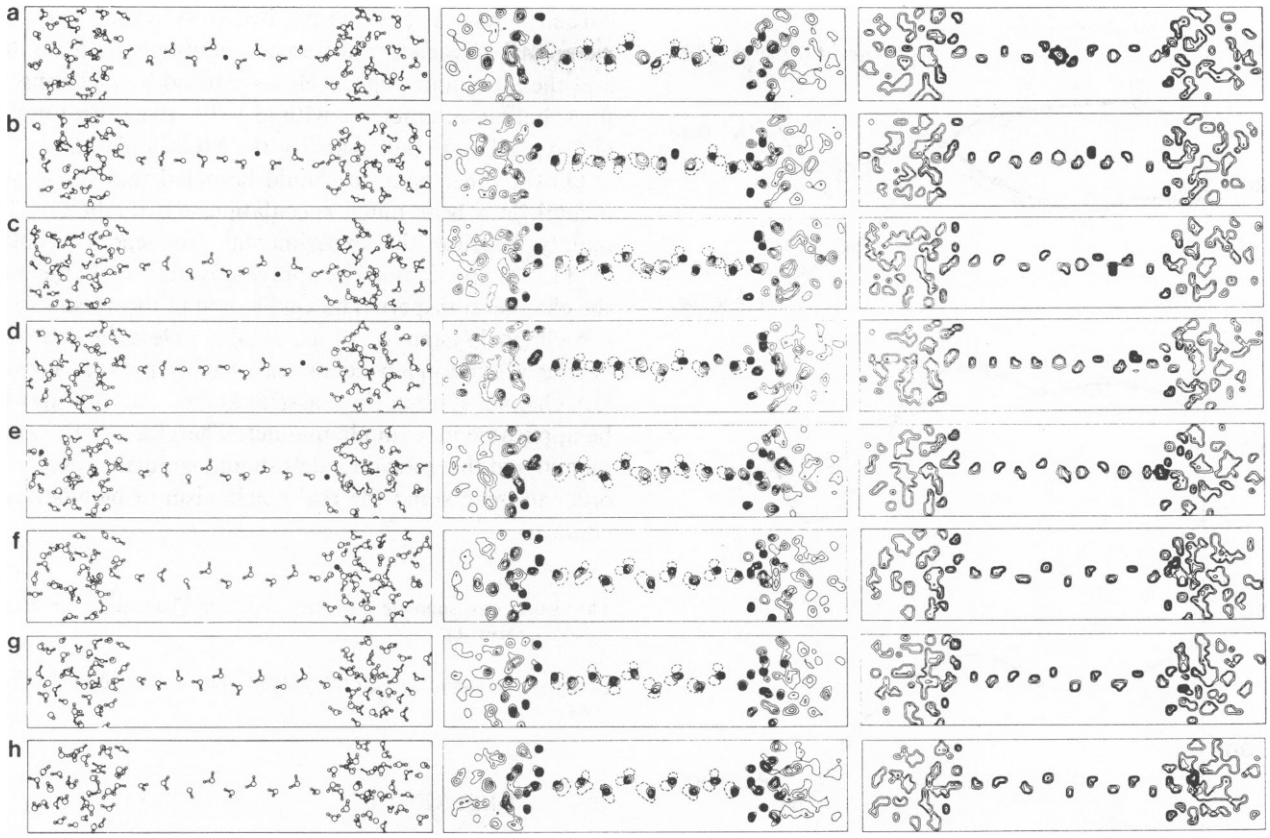

FIGURE 9 Ensemble average positions (first column), probability density maps (second column) and iso-energy density maps (third column) of water molecules obtained by MC simulations for the cases that the average Z position of K^+ is (*a*) −0.8, (*b*) 2.7, (*c*) 6.1, (*d*) 7.9, (*e*) 11.4, (*f*) 13.3, (*g*) 15.0, and (*h*) 16.4 Å, respectively.

particular, the entropy is greater when K^+ is outside the channel because here K^+ is more mobile than when K^+ is inside the channel. On the other hand, when K^+ is outside the channel, the water outside the channel is less mobile due to the strong solvation with the ion, compared to when K^+ is inside the channel. Although the entropy contribution from the water molecules outside the channel and that from the cation have opposite signs, water molecules in the first and second solvation shells are strongly bound to K^+, the entropy decrease of water due to the solvation of the cation expected to be more important; this is particularly true for our simulations owing to the simplified model.

In fact, when K^+ is solvated, the experimental solvation energy (10) is reduced by 22 kJ/mol due to the entropy effects. In our model, the upper bound of the reduction of the solvation energy due to the entropy effects can be estimated to be < 50 kJ/mol by considering an extreme case that all the water molecules solvating the cation were frozen. Because water-water interactions along the X and Y directions were not properly considered due to an

TABLE II
ENERGETICS OF A K^+-WATER-GA SYSTEM

	Z (K^+)	Tot	K^+/T	K^+/GA	½ K^+/W	W/T	W/GA	W/W	Tot/No.	SD
a	−0.8	−6,624	−361	−210	−151	−6,264	−4,004	−2,109	−81.8	0.23
b	2.7	−6,648	−347	−209	−139	−6,301	−4,059	−2,104	−82.1	0.28
c	6.1	−6,651	−354	−210	−144	−6,297	−3,975	−2,178	−82.1	0.27
d	7.9	−6,631	−342	−197	−146	−6,288	−3,998	−2,146	−81.9	0.29
e	11.4	−6,658	−367	−169	−198	−6,291	−3,934	−2,159	−82.2	0.28
f	13.3	−6,695	−431	−186	−246	−6,263	−3,950	−2,067	−82.7	0.29
g	15.0	−6,742	−448	−187	−261	−6,295	−3,957	−2,076	−83.2	0.35
h	16.4	−6,718	−396	−110	−285	−6,321	−4,042	−1,995	−82.9	0.48

Z coordinates of K^+, [Z(K^+)], total energy of the system (Tot), energy components contributed from K^+ (K^+/T, K^+/GA, K^+/W for total, GA, water, respectively), energy components contributed from water (W/T, W/GA, W/W for total, GA, water, respectively), total energy of the system per mol-water (Tot/No.), and standard deviation of the K^+ ion position (SD). (Energies are reported in kilojoules, while Z and SD are in ångströms.)

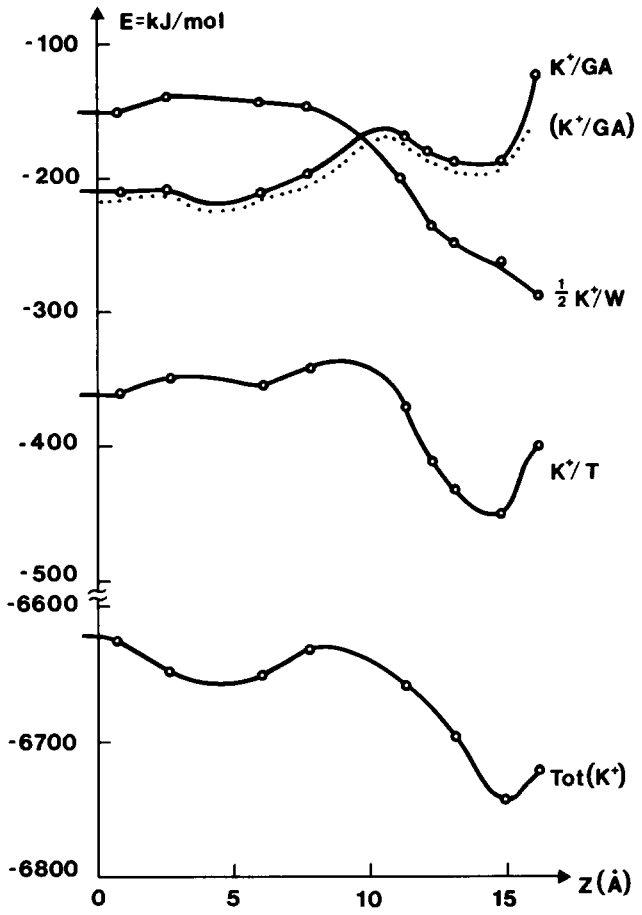

FIGURE 10 Energy profiles obtained by MC simulations for K^+ interacting with the solvated GA. K^+/GA amd K^+/W represent the contributions to the interaction energy from K^+ with GA and from K^+ with water, respectively; while K^+/T represents the total interaction energy from K^+ ($K^+/T = K^+/GA + \frac{1}{2} K^+/W$). The total energy of the K^+-water-GA system is represented by Tot. The dotted line denoted by (K^+/GA) is for the case without solvation and thermal correction (see the energy profile in Fig. 7).

imposed hard wall, most water molecules solvating the cation oriented toward the cation, especially when the cation was outside the channel.

Therefore, the free energy difference between the maximum and the minimum can be in the range of 70–100 kJ/mol, whereas the internal energy activation barrier can be in the range of 20–50 kJ/mol. This rough estimation can be compared with the experimental data (1, 11, 12): the free energy difference between the maximum and the minimum is 30–40 kJ/mol, the free energy activiation barrier is 20–30 kJ/mol, and there is one maximum at $Z = 0$ Å and two minima (one near $Z = 11$ Å and the other near the outside of the channel mouth). The comparison between our results and experimental results indicate that the solvation energy outside the channel was overestimated. The first minimum position detected by experiment is called a binding site. To realize this binding site, the theoretical model needs to include the libration of the carbonyl oxygens and the tail hydroxyl oxygen. Also, the calculated free energy difference between the maximum and the minimum might well be reduced by including the phospholipid interactions with GA, the dynamical motion of GA, and more bulk water in the MC simulation.

On the other hand, it should be noted that the experimental data bear much speculation and doubt (13, 14), mainly because the experimental free energy profiles (1, 11, 12) are obtained by applying Eyring's rate theory to the channel transport. The application of this theory to the GA channel system is not too reliable unless the activation barrier is time independent and sharply peaked. For this GA channel system, the classical kinetic theories may not be applicable in a simple manner. Therefore, both experimental and theoretical models should be further evolved in order to understand the real mechanism of biomembrane channels.

This work was supported by the National Foundation for Cancer Research (NFCR).

Received for publication 21 May 1984 and in final form 4 October 1984.

REFERENCES

1. Urry, D. W. 1982. On the molecular structure and ion transport mechanism of the gramicidin transmembrane channel. *In* Membranes and Transport, Vol. 2. A. N. Martonosi, editor. Plenum Publishing Corp., New York. 285–294.
2. Ovchinnikov, Y. A., and V. T. Ivanov. 1982. Helical structures of gramicidin A and their role in ion channeling. *In* Conformation in Biology. R. Srinivasan and R. H. Sarma, editors. Adenine Press, New York. 155–174.
3. Fornili, L. S., D. P. Vercauteren, and E. Clementi. 1984. Water structure in the gramicidin A transmembrane channel. *J. Biomolec. Struct. Dynam.* 1:1281–1297.
4. Urry, D. W., T. L. Trapane, and K. U. Prasad. 1982. Molecular structure and ionic mechanisms of an ion-selective transmembrane channel: monovalent versus divalent cation selectivity. *Int. J. Quant. Chem. Quant. Biol. Symp.* 9:31–40.
5. Gianclio, L., R. Pavani, and E. Clementi. 1978. A new algorithm for obtaining contracted basis set from gaussian type functions. *Gazz. Chim. Ital.* 108:181–205.
6. Clementi, E., F. Cavallone, and R. Scordamaglia. 1977. Analytical potential from ab initio computations for the interactions between biomolecules. I. Water with amino acids. *J. Am. Chem. Soc.* 99:5531–5545.
7. Clementi, E., G. Corongiu, and G. Ranghino. 1981. Analytical potential from ab initio computations for the interaction between biomolecules. VII. Polar amino acids and conclusions. *J. Chem. Phys.* 74:578–588.
8. Mulliken, R. S. 1955. Electronic population analysis on LCAO-MO molecular wave functions I. *J. Chem. Phys.* 23:1833–1840.
9. Metropolis, N., A. W. Rosenbluth, M. N. Rosenbluth, A. H. Teller, and E. Teller. 1953. Equation of state calculations by fast computing machines. *J. Chem. Phys.* 21:1087–1092.
10. Friedman H. L., and C. V. Krishnan. 1979. Thermodynamics of Ionic Hydration. *In* Water: A Comprehensive Treatise. Vol. 3. F. Franks, editor. Plenum Press, New York. 1–118.
11. Eisenman, G., and J. P. Sandblom. 1984. Modeling the gramicidin

channel: interpretation of experimental data using rate theory. *Biophys. J.* 45:88–90.

12. Hladky, S. B., and D. A. Haydon. 1972. Ion transfers across lipid membranes in the presence of gramicidin A. *Biochim. Biophys. Acta.* 274:294–312.
13. Lauger, P., W. Stephan, and E. Frehland. 1980. Fluctuations of barrier structure in ionic channels. *Biochim. Biophys. Acta.* 602:167–180.
14. Levitt, D. G. 1982. Comparison of Nernst-Planck and reaction rate models for multiply occupied channels. *Biophys. J.* 37:575–587.